Fission probability calculations for heavy-ion induced reactions*

Hugues Delagrange, Alain Fleury, and John M. Alexander
Centre d'Etudes Nucléaires de Bordeaux-Gradignan, Laboratoire de Chimie Nucléaire ERA No. 144, Le Haut-Vigneau, 33170 Gradignan, France
and Department of Chemistry, State University of New York at Stony Brook, Stony Brook, New York 11794
(Received 8 February 1977)

The Bohr-Wheeler formalism for nuclear fission has been included in a nuclear evaporation code. The added parameters are the saddle-point level density a_f and the fission barrier for $J = 0$, B_f. Effects of ^{4}He evaporation are explored by variation of the relevant level density parameter a_α. Good fits to fission excitation functions could be achieved but ambiguity remains due to the entrance channel, i.e., the estimated critical angular momentum and the α evaporation probability. Three different systems have been investigated: $^{182}W + {}^{12}C \rightarrow {}^{194}Hg$, $^{175}Lu + {}^{12}C \rightarrow {}^{187}Ir$, and $^{174}Yb + {}^{12}C \rightarrow {}^{186}Os$. In this framework the measurement of cross sections for α emission and evaporation residues, as well as that for fission, would suffice to fix the important parameters.

[NUCLEAR REACTIONS, FISSION $^{182}W(^{12}C, f)$; $^{175}Lu(^{12}C, f)$; $^{174}Yb(^{12}C, f)$; calculated fission excitation functions; dependence on l_{crit}, a_f/a_n, a_α/a_n, B_f.]

I. INTRODUCTION

Deexcitation of nuclei produced in heavy-ion-induced reactions generally involves a large range of excitation energy and angular momentum in the continuum. α emission[1] and fission are useful probes to study particular zones in the (E, J) plane.[2] Many experimental results[3-10] show that the fission probability for medium-mass isotopes is emphasized at the larger energies and angular momenta. Usually fission excitation functions rise monotonically and relatively rapidly. This suggests first-chance fission is preponderant and for this situation the experimental fission cross section is not integrated over a long deexcitation chain. Therefore calculations of fission excitation functions must take into account very carefully critical angular momenta for fusion and competition between various deexcitation paths at high energy and high angular momentum. In particular, special attention has to be devoted to α emission.

In the statistical analysis of fission decay two parameters are of great importance: (1) the fission barrier B_f for zero angular momentum, (2) the ratio a_f/a_n of the level density parameters for the saddle-point configuration and the residual nucleus after neutron evaporation. Several authors[11] have extracted these parameters from fission excitation functions. Sikkeland *et al.*[9] fitted the average ratio of fission width to neutron width, with an analytical expression simply considering angular momentum via a rotational energy. In a more elaborate calculation, Plasil and Blann[12] have introduced the J dependence of a rotating liquid-drop model for ground state and saddle-point yrast energies. For light-particle-induced fission, Moretto[13] has presented a general method to investigate shell and pairing effects. More recently, Hagelund and Jensen[14] have improved the theoretical state densities by including "collective enhancements." These calculations generally do not fit the whole energy range of the experimental fission excitation functions.

In this article we have undertaken calculations of fission excitation functions with a sophisticated evaporation code. Various open channels in the deexcitation of high spin nuclei have been counted by numerical integrations. We explore in particular the influence of critical angular momentum and α emission. For several different conditions, the values of the parameters B_f and a_f/a_n were extracted by the fit to fission excitation functions.

In Sec. II, the principal features of the code will be described. The J dependence of different yrast energies and fission barriers are taken from the model of Cohen, Plasil, and Swiatecki[15] (CPS in the following text). Shell effects are included in the level densities and yrast energies. We have used different models to estimate the critical angular momenta.

In Sec. III, the calculated results are presented. The influence of different parameters on the fits to experimental fission cross sections is discussed. The sensitivity of the overall shape of the calculated fission excitation functions to these parameters is also shown. Three different systems are investigated[9]: $^{12}C + {}^{182}W$, $^{12}C + {}^{175}Lu$, and $^{12}C + {}^{174}Yb$. The influence of the level-density parameters a_f/a_n and a_α/a_n is pointed out. The

last section gives conclusions and several possible directions for the improvement of the calculations.

II. FRAMEWORK OF THE CALCULATION

A. Decay rates

Compound nuclei deexcite mainly by evaporation of neutrons, light charged particles (H, He), γ rays, and fission. The statistical model enables us to calculate the different emission widths. The computations have been made with the code GRØGI 2.[16] This code has been described elsewhere.[17] The code is modified to incorporate the fission exit channel. The fission width is calculated via the Bohr and Wheeler formula.[18] Transmission coefficients above the fission barrier are set to one and zero under. Below are summarized the different decay rates R^ν for particles ($\nu = n, p, \alpha$) from an initial state E, J to a final state E_f, J_f:

$$R^\nu(E,J;E_f,J_f)=\frac{1}{h}\frac{\rho^\nu(E_f,J_f)}{\rho(E,J)}\sum_{S=|J_f-s|}^{J_f+s}\sum_{l=|J-S|}^{J+S}T_l^{(\nu)}(\epsilon_\nu) \tag{1}$$

with

$$E_f=E-B^\nu-\epsilon_\nu . \tag{2}$$

ϵ_ν is the kinetic energy of the emitted particle with spin s; B^ν is the binding energy of the emitted particle. Binding energy values were taken from Wapstra and Gove.[19] The transmission coefficients $T_l(\epsilon_\nu)$ were taken from the tables of Mani, Melkanoff, and Iori[20] for neutron and proton emission. For α emission, the table of Huizenga and Igo[21] was used.

For γ-ray decay rates (dipole and quadrupole only) we use

$$R_L^\gamma(E,J;E_f,J_f)=\frac{1}{\hbar}\xi_L\epsilon_\gamma^{2L+1}\frac{\rho_\gamma(E_f,J_f)}{\rho(E,J)} \tag{3}$$

and

$$R^\gamma(E,J;E_f,J_f)=\sum_L R_L^\gamma(E,J;E_f,J_f) \tag{4}$$

$$E_f=E-\epsilon_\gamma , \tag{5}$$

where ξ_L is a normalization constant for photon emission.[16,17]

For fission decay rates we use

$$R^f(E,J)=\frac{1}{h}\frac{1}{\rho(E,J)}\int_0^{E-E_{\rm sad}}\rho_{\rm sad}(E-E_{\rm sad}-K,J)dK , \tag{6}$$

where K is the relative kinetic energy of the two nascent fragments at the saddle point.

B. Level densities and level density parameters

In Eqs. (1)–(6), the quantities ρ, $\rho_{\rm sad}$, and ρ^ν are the level densities of, respectively, the initial nucleus deformed as in its ground state, the initial nucleus at the saddle point configuration, and the residual nucleus after particle emission. Level densities were calculated following the Lang prescription[22]

$$\rho(E,J)=\omega(E,M=J)-\omega(E,M=J+1) , \tag{7}$$

$$\omega(E,M)=\omega(E-M^2/aR\ ,0)\simeq\omega(E-E_{\rm yrast}\ ,0) , \tag{8}$$

$$\omega(E,0)=K\exp(2\sqrt{aU})/R^{1/2}a^2t^3 , \tag{9}$$

$$U=E-\delta=at^2-\tfrac{3}{2}t \tag{10}$$

with δ—the pairing correction, U—the effective excitation energy, and t—the nuclear temperature.

The level-density parameter a was taken from the formula given by Gilbert and Cameron[23]

$$a/A=0.120+0.00917S \tag{11}$$

with A, the mass number and S, the shell correction. The spin parameter R is related to the moment of inertia $\mathcal{I}$ as follows:

$$\mathcal{I}=\frac{aR}{2} . \tag{12}$$

In a similar way, the level density at the saddle point is given by the following set of equations:

$$\rho_{\rm sad}(E_f,J)=\omega_{\rm sad}(E_f,M=J)-\omega_{\rm sad}(E_f,M=J+1) , \tag{13}$$

$$E_f=E-E_{\rm sad}-K , \tag{14}$$

$$\omega_{\rm sad}(E_f,M=J)\simeq\omega_{\rm sad}[E_f'-E_{\rm sad}(J),0] , \tag{15}$$

$$E_f'=E-K , \tag{16}$$

$$\omega(E,0)=K\exp[2(a_fU_f)^{1/2}]/R_f^{1/2}a_f^2t_f^3 , \tag{17}$$

$$U_f=E_f-\delta_f=at_f^2-\tfrac{3}{2}t_f , \tag{18}$$

$$\mathcal{I}_f=\frac{a_fR_f}{2} . \tag{19}$$

The parameters used in Eqs. (17)–(19) are similar to those of Eqs. (9)–(12). For the saddle point, the pairing energy is taken to be equal to the ground-state pairing correction.

The level-density parameters for ground-state configurations have been extracted by Gilbert and Cameron[23] from neutron resonance studies. That means for excitation energies close to neutron binding energies (≈8 MeV) and low spins. However, fission and α emission occur at high angular momenta and high excitation energies. Therefore, a_α and a_f have been taken as free parameters as expressed by the ratios a_α/a_n and a_f/a_n. We try to point out the influence of these two parameters on the resulting value of the fission barrier height. Binding energies of particles and transmission coefficients for α emission have been taken as fixed.

C. Shell effects for yrast energies and fission barriers

Involved calculations of nuclear potential energy surfaces for high angular momenta are in a state of evolution.[24,25] But these modern techniques have not yet been applied to the evolution of the saddle-point configuration with J. However, it is important for both fission barriers and yrast energies to combine the liquid-drop features and those for shell effects.

Liquid-drop calculations (CPS, Ref. 15) give the J dependence of the minimum energies of the ground-state and of saddle-point shapes. The resulting fission barrier is a decreasing function of angular momentum and it vanishes for $Z \approx 80$ at J values of $\approx 60-70\hbar$. However, the CPS method does not include shell effects. For this purpose, the zero-spin fission barrier B_f is considered as an adjustable parameter and the J dependence of the fission barrier is obtained from the following equation:

$$B_f(J) = \frac{B_f(J=0)}{B_f^{\mathrm{CPS}}(J=0)} B_f^{\mathrm{CPS}}(J) . \tag{20}$$

This equation states that the evolution of the fission barrier as a function of J (and the value at which it goes to zero) is the same as in CPS calculation.

Hillman and Grover[26] numerically compute individual yrast energies E_J^{HG} by considering two kinds of interacting fermions (BCS approximation). An average effective moment of inertia $\mathcal{I}^{\mathrm{HG}}$ and pairing correction δ^{HG} can be extracted by a least square fit of a parabola to these yrast energies plotted versus J:

$$E_J^{\mathrm{HG}} = \frac{(J+\frac{1}{2})^2\hbar^2}{2\mathcal{I}^{\mathrm{HG}}} + \delta^{\mathrm{HG}} . \tag{21}$$

This moment of inertia depends strongly on Z and A of the nucleus relative to the closed shells.[27] This shell effect is introduced in our calculations by the following prescription for alteration of the liquid-drop values:

$$E_{\mathrm{yrast}} = E_{\mathrm{min}}(J) = K_{\mathcal{I}} E_{\mathrm{min}}^{\mathrm{CPS}}(J) + \delta^{\mathrm{HG}} , \tag{22}$$

where

$$K_{\mathcal{I}} = \frac{\mathcal{I}^{\mathrm{CPS}}}{\mathcal{I}^{\mathrm{HG}}} . \tag{23}$$

The yrast energies at equilibrium deformation $E_{\mathrm{min}}(J)$ are related to the CPS rotational energies of a rotating liquid drop at equilibrium deformation $E_{\mathrm{min}}^{\mathrm{CPS}}(J)$. The quantity $K_{\mathcal{I}}$ is the ratio of the average moment of inertia extracted from the CPS model $\mathcal{I}^{\mathrm{CPS}}$ to the average effective moment of inertia from the shell model $\mathcal{I}^{\mathrm{HG}}$. Yrast energies of the saddle-point shape $E_{\mathrm{sad}}(J)$ are then obtained by the equation

$$E_{\mathrm{sad}}(J) = E_{\mathrm{min}}(J) + B_f(J) . \tag{24}$$

D. Critical angular momenta

The partial-wave reaction cross sections are expressed in the standard way:

$$\sigma_R(E,l) = \pi\lambda^2(2l+1)T_l(\epsilon) \tag{25}$$

and the total reaction cross section from the sum:

$$\sigma_R(E) = \sum_{l=0}^{\infty} \sigma_R(E,l) . \tag{26}$$

In the above equations, transmission coefficients were obtained from the parameters of Vaz and Alexander[28] for the formalism of Wong.[29] The needed parameters are described elsewhere.[30] To calculate the fusion cross sections, we limit the l summation at l equal to the critical angular momentum l_{crit}:

$$\sigma_{\mathrm{fus}}(E) = \sum_{l=0}^{l=l_{\mathrm{crit}}} \sigma_R(E,l) . \tag{27}$$

Since fission takes place at high angular momenta, l_{crit} is an essential parameter. In order to show the influence of the value of this parameter, l_{crit} values were computed in two different ways. For case I, they have been extracted from an empirical formula of Alexander and Lanzafame.[31] For case II, the Bass model[32] has been used. Our purpose here is simply to show the effect of a variation in l_{crit}, not to try to sell either of these recipes.

The available experimental fusion data were correlated by Alexander and Lanzafame (1973) in terms of the ratio of the fusion cross sections σ_{fus} and the total reaction cross section σ_R, and the ratio of the incident energy ($E_{\mathrm{c.m.}}$) to the classical Coulomb barrier V:

$$\left(\frac{\sigma_{\mathrm{fus}}}{\sigma_R}\right) = 1.99146 - 1.39066\left(\frac{E_{\mathrm{c.m.}}}{V}\right) + 0.469937\left(\frac{E_{\mathrm{c.m.}}}{V}\right)^2 - 0.073472\left(\frac{E_{\mathrm{c.m.}}}{V}\right)^3 + 0.00411099\left(\frac{E_{\mathrm{c.m.}}}{V}\right)^4 . \tag{28}$$

Bass employed a potential between the two colliding nuclei $V_l(r)$ that includes a centrifugal potential, a Coulomb potential, and a nuclear two body potential:

$$V_l(r) = \frac{Z_1 Z_2 e^2}{r} + \frac{\hbar^2 l^2}{2\mu r^2} - a_s A_1^{1/3} A_2^{1/3} \times \frac{d}{R_{12}} \exp - \left(\frac{r - R_{12}}{d}\right) . \tag{29}$$

In this equation, Z and A are atomic number and mass number, and μ is the reduced mass. The index 1 stands for the projectile and the index 2 for the target. The distance between the centers of the two spherical colliding nuclei is r, and R_{12} is the sum of the radii at the half-maximum density. This radius R_{12} is $R_{12}=R_1+R_2=r_0(A_1^{1/3}+A_2^{1/3})$ with $r_0=1.07$ fm; a_s is the surface coefficient in the liquid-drop-model mass formula ($a_s=17.0$ MeV), and d is the nuclear force range, obtained by a fit to the experimental interaction barriers ($d=1.35$ fm).

At low incident energies, the critical angular momentum is obtained by setting the potential $V_l(r)$ equal to the incident energy, $E_{c.m.}=V_l$ at a distance R_{max} corresponding to the maximum of the potential. When the incident energy is increased, the value of R_{max} decreases and is equal to R_{12} at $E_{c.m.}=E_1$. At energies greater than E_1, the limiting angular momentum is given by the following equation:

$$l_{crit}(\hbar)=\left[2\mu R_{12}^2\left(E_{c.m.}-\frac{Z_1Z_2e^2}{R_{12}}+da_s\frac{A_1^{1/3}A_2^{1/3}}{R_{12}}\right)\right]^{1/2}. \quad (30)$$

The third energetic zone where complete dissipation of the radial kinetic energy leads to an asymptotic value of the fusion l_{crit}, is never reached in the three reactions considered.

In Table I, the calculated l_{crit} values are summarized for the reaction $^{182}W+^{12}C$. At low energies the results are quite similar for the two different models, however the differences are quite notable at higher energies. These features are analyzed in the next section.

TABLE I. Values of l_{crit} deduced from two different models for $^{182}W+^{12}C$.

E_{lab} (MeV)	$E_{c.m.}$ (MeV)	l_{crit} (case I)[a]	l_{crit} (case II)[b]
70.8	66.4	28	28
74.3	69.7	30	31
77.9	73.1	33	34
82.7	77.6	35	37
88.1	82.7	38	40
90.6	85.0	38	41
93.2	87.4	39	43
98.2	92.1	41	45
102.8	96.4	42	47
107.8	101.1	43	49
109.7	102.9	44	50
111.8	104.9	44	51
116.3	109.1	45	53
120.2	112.8	46	54
124.6	116.9	47	55

[a]Reference 31. [b]Reference 32.

III. RESULTS AND ANALYSIS

For a given set of initial parameters ($a_\gamma, a_n, a_p, a_\alpha, l_{crit}$), the best fit to the experimental fission excitation functions is obtained by varying only the fission parameters a_f/a_n and B_f. The influence of some initial parameters was explored by changing the value of one parameter at a time and then the procedure was repeated to obtain another set of parameters ($a_f/a_n, B_f$).

Only the two first steps of the neutron decay chain were considered. The fission parameters ($B_f, a_f/a_n$) for the ($A-1$) nucleus were taken as equal to those for the A nucleus. The calculated second-chance fission represents never more than 40% of that for first-chance fission (Fig. 1) and is on the average about 20%. The theoretical values for the fission barriers for the ($A-1$) nucleus are quite close to those for the A nucleus and this seemed to be a reasonable choice given our present state of knowledge.

A. Fission parameters: Uniqueness

For a set of initial parameters the first question is to know if the solution for the fission parameters is unique. A trial analysis has been made for the reaction $^{182}W+^{12}C\rightarrow{}^{194}Hg$. Calculations have been performed with critical angular momenta of case I and the level-density parameters of Eq. (11). The influence of a_f/a_n and B_f on the fission excitation function is presented on Figs. 2(a) and 3(a). The ratio of computed to best-fit cross sections are displayed in Figs. 2(b), 3(b), and 4 for three different cases. These figures show the influence of each parameter for the complete energy range of the fission excitation functions. Three different cases are discussed below.

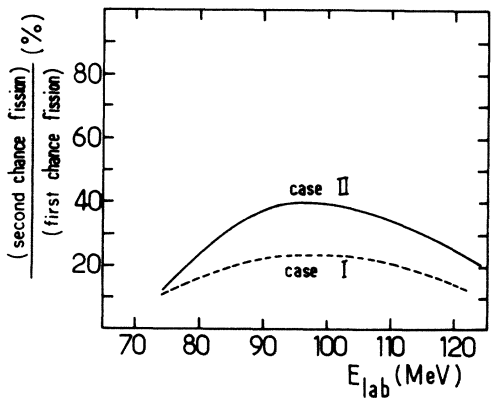

FIG. 1. Ratio of calculated second-chance fission to calculated first-chance fission. This ratio has been calculated with l_{crit} from cases I and II. Level-density parameters are from Eq. (11).

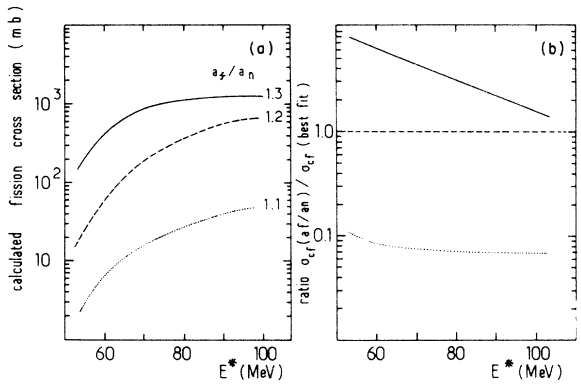

FIG. 2. Influence of the parameter a_f/a_n on the calculated fission cross sections for the system $^{182}W+^{12}C \rightarrow ^{194}Hg$: a_f/a_n, =1.3 (solid curve), 1.2 (best fit, dashed curve), 1.1 (dot curve). l_{crit} is from case I, and level densities are from Eq. (11). The fission barrier is the best-fit value 17.5 MeV. Figure 2(b) compares the different cross sections to the best-fit ones. Best fits are shown in Fig. 6.

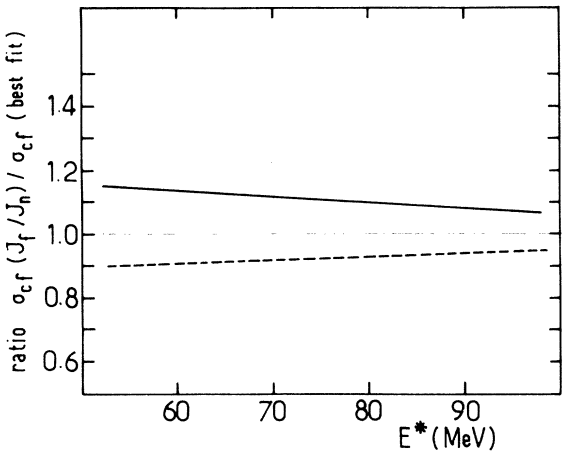

FIG. 4. Influence of g_f/g_0. Calculated fission cross sections for $g_f/g_0=1.5$ (solid curve) and for $g_f/g_0=2.5$ (dashed curve) are compared with best-fit value of $g_f/g_0=2$. The fission parameters are $a_f/a_n=1.2$ and $B_f=17.5$.

The first parameter studied is the level-density parameter a_f at the saddle point; it is expressed in the form a_f/a_n. Figure 2(a) shows clearly the very important variations of the calculated fission cross sections with this parameter. Due to this very great sensitivity to a_f/a_n the parameter can be fixed rather precisely by the fit largely independent of the other parameters. Excitation function shapes as well as the absolute fission cross sections depend on a_f/a_n. For a_f/a_n values smaller than 1.2, the shapes are very similar. For a_f/a_n values greater than 1.2 the fission excitation functions become flatter.

The influence of B_f on the calculated cross sections is less spectacular but still very important (Fig. 3). A variation of 1 or 2 MeV on the value of B_f induces a change at low energies of more than 50% in the calculated cross sections. Thus, the best-fit value of B_f will also be quite precise. In Fig. 3(b) are shown modifications in the shape of the fission excitation functions when B_f is varied around the "best-fit" values. The slope of the fission excitation function is increased when B_f values become larger.

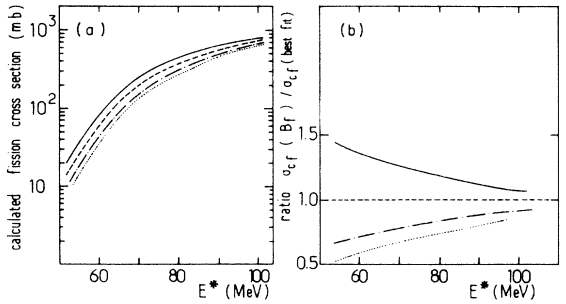

FIG. 3. Influence of the fission barrier height on calculated fission cross sections for $^{182}W+^{12}C \rightarrow ^{194}Hg$. Four values of B_f have been used: 17.0 MeV (solid curve), best fit 17.5 MeV (dashed curve), 18.0 MeV (dot-dashed curve), 18.3 MeV (dot curve). The parameter a_f/a_n is the best-fit value, $a_f/a_n=1.2$. The remaining parameters are described in Fig. 2. Figure 3(b) compares the different curves to that for the best fit.

The parameter g_f/g_0 has only a small influence on the calculated fission cross sections. The knowledge of this quantity is only relevant to the fission spin parameter R_f in the denominator of Eq. (17). In Fig. 4 we see that a change in g_f/g_0 of 25% changes the calculated cross sections slightly over the whole energy range considered. Later we choose g_f/g_0 as constant and equal to 2.

From the pattern above we can discuss the best-fit couple for $(a_f/a_n, B_f)$. In Fig. 5 are plotted the χ^2 values versus the fission parameters B_f and a_f/a_n. There are two possibilities to search for another best fit. If B_f is decreased, fission cross sections are increased and the excitation functions flattened. To compensate for this effect, the ratio a_f/a_n must be lowered. In this direction of the $(B_f, a_f/a_n)$ plane the χ^2 values rise rapidly and no other fit could be found. On the other hand we could try to increase B_f. Then fission cross sections are decreased and the excitation function rises more sharply than the experimental one. The parameter a_f/a_n must be increased and the excitation function is flattened. The two effects partially compensate but nevertheless the compensation is never complete. The χ^2 values increase more slowly in this direction. The two preceding

conclusions illustrate the overall χ^2 hypersurface. A valley goes down from large a_f/a_n and B_f to a well pronounced minimum. Estimated uncertainties are of the order of 0.1 MeV for B_f and of 0.01 for a_f/a_n.

B. Fusion cross section influence: Application to different systems

Fission excitation functions have been measured by Sikkeland and co-workers[9] for the following three systems, $^{182}W+^{12}C \rightarrow ^{194}Hg$, $^{175}Lu+^{12}C \rightarrow ^{187}Ir$, and $^{174}Yb+^{12}C \rightarrow ^{186}Os$. We have treated these reactions because the compound nuclei have similar mass numbers but the fission cross sections are quite different. Successful fits to these different fission excitation functions provide a test of the sensitivity of the calculations. For the system leading to ^{194}Hg, at 77.9 MeV bombarding energy, the fission cross section is 24.2 mb, for ^{187}Ir it is ~1.9 mb and for ^{186}Os it is only about ~0.4 mb. For 120.2 MeV incident energy, the values are, respectively, 745, 220, and 93.1 mb.

For each of these systems the statistical parameters used in the calculations are listed in Table II. As previously discussed two different sets of l_{crit} have been investigated. Figures 6–8 show the good quality of fits obtained even for the low fission cross sections. The parameters are summarized in Table III. Theoretical B_f values obtained by Myers and Swiatecki[33] and by Cohen, Plasil, and Swiatecki are included for comparison in this table.

Independent analysis of ^{4}He-induced ^{186}Os fission probabilities give, respectively, for B_f, 23.4 MeV[13,34] and 22.5 MeV.[14] These values are in fairly good agreement with the values in Table III. These fits also are reasonably close to the theoretical barrier heights. However, as the values of l_{crit} are not well known it is difficult to define B_f

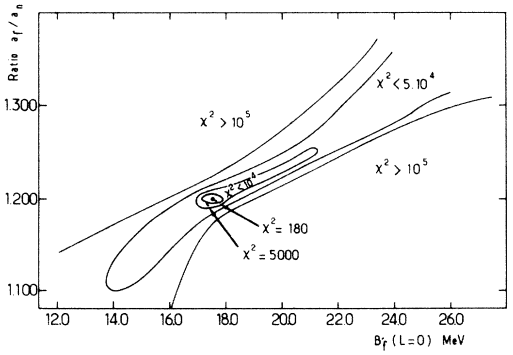

FIG. 5. Contour plots describing the variation of χ^2 versus the fission parameters. The values of l_{crit} are from case I and level-density parameters are from Eq. (11).

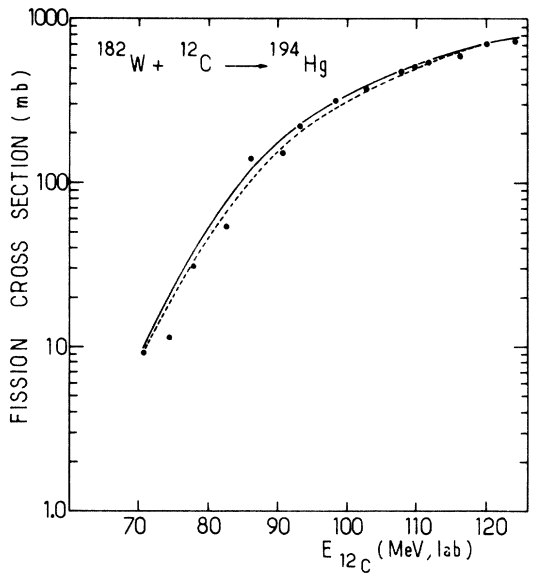

FIG. 6. Fission excitation function for $^{182}W+^{12}C \rightarrow ^{194}Hg$. Points are the experimental data from Ref. 9. The solid curve corresponds to calculations carried out with l_{crit}, from case I; the dashed curve from case II.

with a better accuracy than ±1.5 MeV. Consequently we are not able to choose between the fission barriers calculated in Refs. 15 and 33. Usually our values are between these two theoretical values.

C. Influence of the parameter a_α/a_n

α emission is crucial at high excitations and the compound-nucleus decay is mainly governed by the competition of α emission and fission. Level-density parameters given by Eq. (11) lead to a ratio a_α/a_n of 1.09 in the decay of ^{194}Hg. To investigate the influence of this parameter we have considered an extreme case, namely, $a_\alpha/a_n = 1.0$. For this case with no change in the other parameters, the calculated fission cross sections are larger than the experimental ones. To reach again a best fit, the general procedure explained above was applied. A new best fit was achieved with fission parameters of $a_f/a_n = 1.12$ and $B_f = 15.5$ MeV. These two values are given in Table III. These effects are shown in Fig. 9. Let us briefly describe this figure. In Fig. 9(a) are plotted particle-emission and fission excitation functions for the first two steps of the decay chain. The parameters for the calculation were l_{crit} values from the Bass model, level-density parameters from Eq. (11), and the relevant fission parameters (see Table III). Neutron emission is the leading decay channel at low incident energies. Neutron, α-emission, and fission cross sections have similar val-

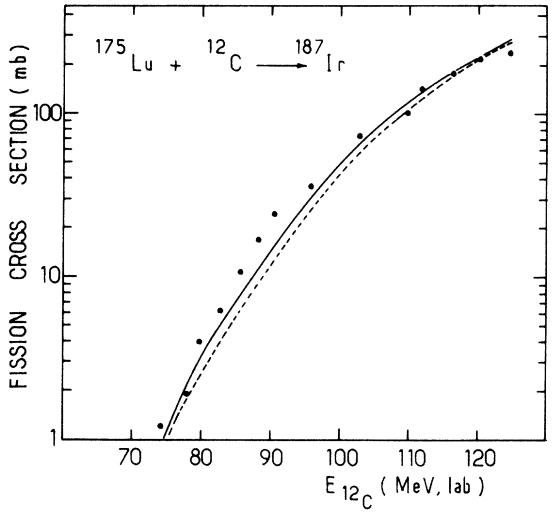

FIG. 7. Fission excitation function for ^{175}Lu + ^{12}C → ^{187}Ir. Notation as in Fig. 6.

ues at high bombarding energies. Proton cross sections never reach more than 36 mb for the whole energy range considered. Figure 9(b) displays the same cross sections but with a_α/a_n equal 1.0 and fission parameters refitted (see Table III). This decrease in the α-emission cross section leads to a larger increase for the neutron emission than for the protons. Simultaneously, at 120.2 MeV, α cross sections go from 639 to 81 mb. Calculated fission barriers are then very dependent on the α-fission competition at high J.

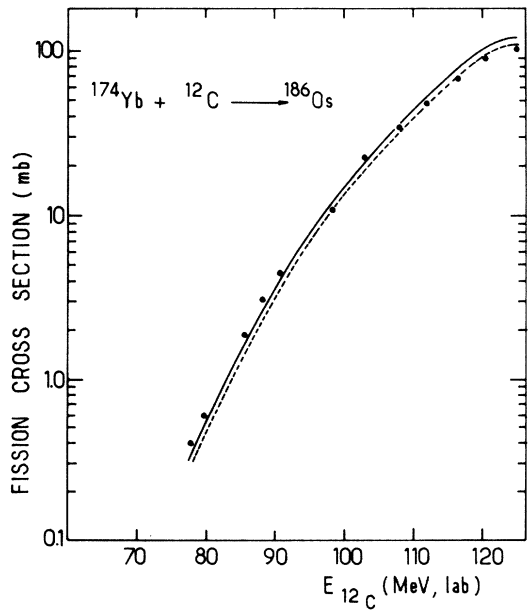

FIG. 8. Fission excitation function for the system ^{174}Yb + ^{12}C → ^{186}Os. Notation as in Fig. 6.

TABLE II. Level-density parameters used in the calculations.

A	a (MeV^{-1})	δ (MeV)	g_{rig}/g_{eff}
		Hg isotopes	
194	19.35	1.82	1.52
193	20.26	0.93	1.27
192	20.33	1.75	1.26
		Au isotopes	
192	21.05	0.67	1.20
191	21.12	1.57	1.19
		Pt isotopes	
190	22.00	1.73	1.27
189	21.95	0.77	1.14
		Ir isotopes	
187	22.42	1.75	1.05
186	22.54	0.59	1.04
185	22.66	1.76	1.05
		Os isotopes	
186	21.88	2.20	1.01
185	22.00	1.24	0.98
184	22.11	2.25	1.00
		Re isotopes	
185	21.35	1.31	0.92
184	21.47	0.04	0.92
183	22.33	1.32	0.91
182	22.00	0.20	0.82
		W isotopes	
182	21.29	1.94	0.85
181	21.70	1.02	0.75

Accurate measurements of α cross sections are obviously needed.

D. Some remarks on the a_f/a_n parameter

For each case considered here, values for a_f/a_n are greater than unity. This indicates that the number of levels involved in the compound nucleus decay are greater for the saddle-point configuration than for the ground-state configuration. That can be understood from two directions. First, on the average, single-particle states have lower energies when the nucleus is well deformed. Thus in the excited nucleus the number of accessible states is greater for a given excitation energy. Secondly, in strongly deformed nuclei (compared with spherical) broken symmetries and collective states[35,36] lead to an increased number of states. All these effects are included in the parameter a_f.

TABLE III. Calculated fission parameters (see text for further details on the other parameters of the calculations).

System	Compound nucleus	$B_f(J=0)$ calculated (MeV)	a_f/a_n calculated	B_f Myers-Swiatecki (Ref. 33)	$B_f(J=0)$ CPS (Ref. 15)
		l_{crit} (case I)[a]			
$^{182}W+^{12}C$	^{194}Hg	17.5	1.20	18.3	15.0
$^{175}Lu+^{12}C$	^{187}Ir	20.1	1.16	21.1	19.3
$^{174}Yb+^{12}C$	^{186}Os	22.8	1.19	23.2	21.2
		l_{crit} (case II)[b]			
$^{182}W+^{12}C$	^{194}Hg	16.5	1.16	18.3	15.0
$^{175}Lu+^{12}C$	^{187}Ir	18.3	1.10	21.1	19.3
$^{174}Yb+^{12}C$	^{186}Os	21.3	1.13	23.2	21.2
		α emission influence $a_\alpha/a_n=1.0$, l_{crit} from Ref. 32			
$^{182}W+^{12}C$	^{194}Hg	15.5	1.12	18.3	15.0

[a] Reference 31. [b] Reference 32.

E. Study of the E-J plane

The different probabilities for particle emission and fission are plotted in Figs. 10 and 11, in the E-J plane, for best-fit fission parameters. Figure 10 corresponds to case I and Fig. 11 case II. Several main features can be deduced from these plots. α particles are mainly emitted at high E and relatively low J. These particles are type I α particles, following the Grover and Gilat[37] nomenclature. It has been shown the presence of this kind of emission is controlled by the values of a_α/a_n[1] (see Table II). Neutron emission is the main deexcitation mode for medium excitation energies and relatively low J. Fission occurs at high E and high J.

α competition is a very important decay mode in the deexcitation of these nuclides. Let us emphasize this point. For an excitation energy of 100 MeV (corresponding to 125 MeV in the lab system for the system $^{12}C+^{182}W$), the main com-

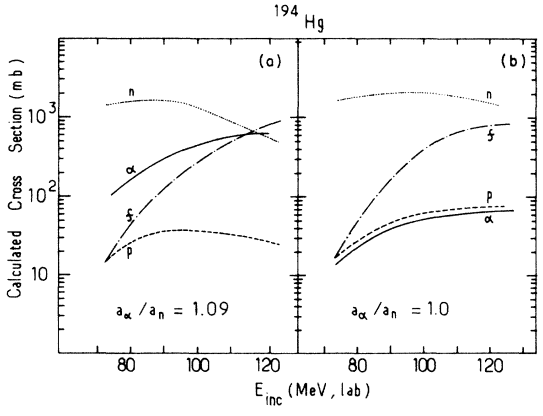

FIG. 9. Fission and n,p,α excitation functions considered for the first two steps of the evaporation case. Both cases were computed with l_{crit} from case II. In Fig. 9(a), level-density parameters were obtained from Eq. (11). In Fig. 9(b), a_α/a_n was taken equal to unity. The solid curve is for α emission, dot curve for neutron emission, dashed curve for proton emission, and dot-dashed for fission.

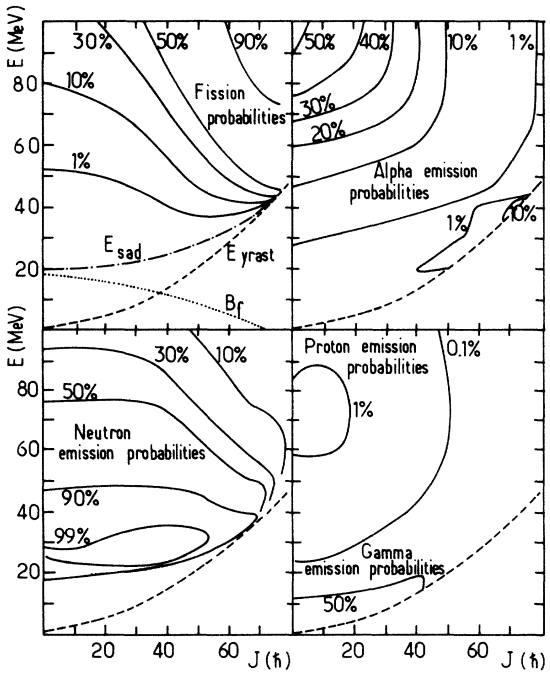

FIG. 10. Emission probabilities for ^{194}Hg nuclei. Fission parameters are the best fit for case I with level-density parameters from Eq. (11).

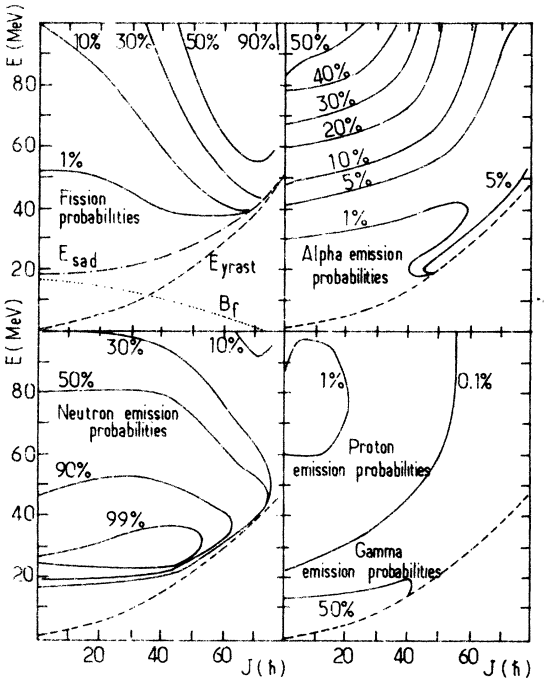

FIG. 11. Emission probabilities for ^{194}Hg nuclei. Fission parameters are the best fit for case II with level-density parameters from Eq. (11).

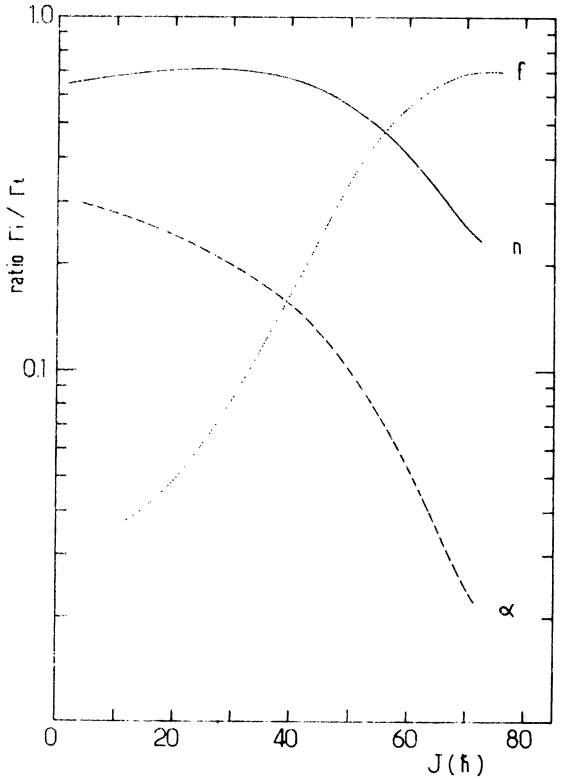

FIG. 12. Calculated partial cross sections for 120 MeV ^{12}C + ^{182}W → ^{194}Hg case II parameters. Reaction cross section (solid curve), α emission (dashed curve), and fission (dot curve).

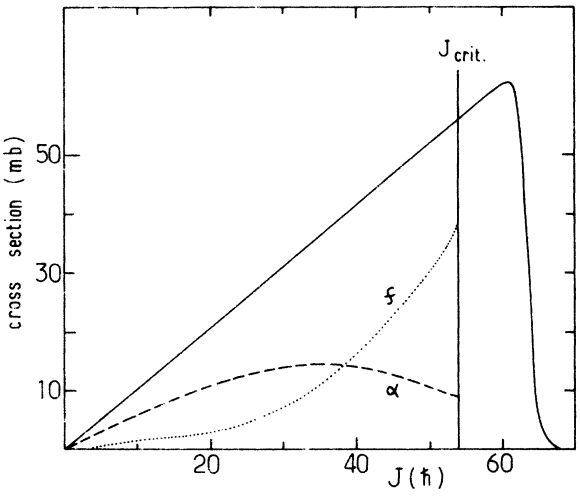

FIG. 13. Particle-emission and fission probabilities calculated with case II parameters at 68 MeV excitation energy.

petition is between α emission and fission. Fission takes over for high J. The effect of α competition on the fission excitation functions is most important at high energy. For medium excitations, the pattern is not so simple. As shown in Fig. 12 (excitation energy of 68 MeV), for low values of the angular momenta, only α and neutron emission are significant. For J around $40\hbar$, neutron emission is still predominant but fission and α emission are also important. For greater values of $J(\approx 65\hbar)$, the situation is quite different; fission is predominant, there remains some neutron emission but α emission gives only a small contribution. Sometimes, this contribution can be high just above the yrast line (type II alpha particles). Finally, Fig. 13 displays calculated cross sections for a bombarding energy of 120.2 MeV, with case II parameters. α cross sections show a slow change with angular momentum while fission cross sections begin to mount rapidly around $30\hbar$.

IV. CONCLUDING REMARKS AND SUMMARY

Statistical deexcitation calculations (for $Z \approx 80$) are able to reproduce fission excitation functions. For a given set of input cross sections or l_{crit} values the fission parameters a_f/a_n and B_f are essentially unique. Our main point is the reproduction of the overall excitation function; the shape of the curve is a high-level constraint. The importance of α-emission and fission competition have been emphasized at high excitation energy. The evapora-

tion code GRØGI 2 is very inclusive but fission parameters do require a more complete experimental investigation of σ_f/σ_α and l_{crit} to be more precisely fixed.

The use of fission excitation functions alone leads to ambiguities in the determination of the fission parameters $(a_f/a_n, B_F)$. Level-density parameters (e.g., a_α) obtained at low excitation energy are not necessarily appropriate for high energies. This feature and the indetermination of l_{crit} limit the accuracy of the fitted fission parameters; they can be obtained with good precision when these quantities are measured. Possibilities to remove these ambiguities are twofold. Firstly, a complete set of measurements including fusion (evaporation residues plus fission) and α-particle-emission cross sections will lead to unambiguous values for critical angular momenta, level-density parameters and fission barriers. Experimental studies on ^{194}Hg are presently underway.[38] Secondly, one should make a deeper attack on the theoretical level densities. One might generate numerical level densities for nuclei at various deformations and thus get better values for level density parameters (a_n, a_α, a_f) or even a better formulation of the level-density relationships.

---

*Work supported in part by l'Institut de Physique Nucléaire et de Physique des Particules and the U. S. Energy Research and Development Administration.

[1]A. Fleury and H. Delagrange, in Proceedings of the European Conference on Nuclear Physics with Heavy Ions, Caen, France, 1976 (unpublished), p. 104.

[2]A. Fleury and J. M. Alexander, Ann. Rev. Nucl. Sci. 24, 279 (1974).

[3]A. M. Zebelman, L. Kowalski, J. M. Miller, K. Beg, Y. Eyal, G. Yaffe, A. Kandil, and D. Logan, Phys. Rev. C 10, 200 (1974).

[4]B. Tamain, These de'Etat, Clermont-Ferrand, 1974 (unpublished).

[5]J. Peter, F. Hanappe, in *Proceedings of the International Conference on Nuclear Physics, Munich, 1973*, edited by J. de Boer and H. J. Mang (North-Holland, Amsterdam/American Elsevier, New York, 1973), Vol. 1.

[6]A. I. Obukhov, N. A. Perfilov, O. E. Shigaev, and E. G. Tkachenko, Yad. Fiz. 11, 977 (1970) [Sov. J. Nucl. Phys. 11, 543 (1970)].

[7]L. Kowalski, A. M. Zebelman, J. M. Miller, G. F. Herzog, and R. C. Reedy, Phys. Rev. C 1, 259 (1970).

[8]T. Sikkeland, Phys. Rev. 135, 669 (1964).

[9]T. Sikkeland, J. E. Clarkson, N. H. Steiger-Shafrir, and V. E. Viola, Phys. Rev. C 3, 329 (1971).

[10]F. Plasil, R. L. Ferguson, and F. Pleasonton, in Proceedings of the IAEA Symposium, New York, 1973 (unpublished).

[11]R. Vandenbosch and J. R. Huizenga, *Nuclear Fission* (Academic, New York, 1973).

[12]F. Plasil and M. Blann, Phys. Rev. C 11, 508 (1975).

[13]L. G. Moretto, in Proceedings of the IAEA Symposium, New York, 1973 (see Ref. 10).

[14]H. Hagelund and A. S. Jensen (unpublished).

[15]S. Cohen, F. Plasil, and W. J. Swiatecki, Ann. Phys. (N.Y.) 82, 557 (1974).

[16]J. R. Grover and J. Gilat, Phys. Rev. 157, 802 (1967).

[17]J. Gilat, Brookhaven National Laboratory Report No. BNL 50246, 1970 (unpublished).

[18]N. Bohr and J. A. Wheeler, Phys. Rev. 56, 426 (1939).

[19]A. H. Wapstra and N. B. Gove, Nucl. Data A9, 265 (1971).

[20]G. S. Mani, M. A. Melkanoff, and I. Iori, CEA Reports Nos. 2379 and 2380, 1963 (unpublished).

[21]J. R. Huizenga and G. I. Igo, Argonne National Laboratory Report No. 6373, 1961 (unpublished).

[22]D. W. Lang, Nucl. Phys. 77, 545 (1966).

[23]A. Gilbert and A. G. W. Cameron, Can. J. Phys. 43, 1446 (1965).

[24]A. Faessler, K. R. Sandhya Devi, F. Grummer, K. W. Schmid, and R. R. Hilton, Nucl. Phys. A256, 106 (1976).

[25]G. Andersson, S. E. Larsson, G. Leander, P. Möller, S. G. Nilsson, I. Ragnarsson, S. Aberg, R. Bengtsson, J. Dudek, B. Nerlo-Pomarska, K. Pomarski, and Z. Szymanski, Nucl. Phys. A268, 205 (1976).

[26]M. Hillman and J. R. Grover, Phys. Rev. 185, 1303 (1969).

[27]H. Delagrange, F. Hubert, and A. Fleury, Nucl. Phys. A228, 397 (1974).

[28]L. C. Vaz and J. M. Alexander, Phys. Rev. C 10, 464 (1974).

[29]C. Y. Wong, Phys. Rev. Lett. 31, 766 (1973).

[30]J. M. Alexander, H. Delagrange, and A. Fleury, Phys. Rev. C 12, 149 (1975).

[31]J. Gilat, E. R. Jones, III, and J. M. Alexander, Phys. Rev. C 7, 1973 (1973).

[32]R. Bass, Nucl. Phys. A231, 45 (1974).

[33]W. Myers and W. F. Swiatecki, Nucl. Phys. 81, 1 (1966).

[34]L. G. Moretto, S. G. Thompson, J. Routti, and R. C. Gatti, Phys. Lett. 386, 471 (1972).

[35]S. Bjørnholm, A. Bohr, and B. R. Mottelson, in Proceedings of the IAEA Symposium, New York, 1973 (see Ref. 10).

[36]A. Bohr and B. R. Mottelson, *Nuclear Structure* (Benjamin, New York, 1975), Vol. II, p. 38.

[37]J. R. Grover and J. Gilat, Phys. Rev. 157, 823 (1967).

[38]J. M. Miller, D. Logan, G. Catchen, M. Rajagopalan, J. M. Alexander, M. Kaplan, M. S. Zisman, and L. Kowalski (unpublished).